Electronic Supporting Information for

Highly Fluorescent Anthracene Derivative as Non-fullerene Acceptor in OSCs with Small Non-radiative Energy Loss of 0.22 eV and High PCEs over 13%

Chao Yao[a], Bin Liu[a], Yanan Zhu[a], Ling Hong[b], Jingshen Miao[a], Jianhui Hou*[b], Feng He*[c], Hong Meng*[a]

[a] School of Advanced Materials, Peking University Shenzhen Graduate School, Shenzhen 518055, China

[b] Beijing National Laboratory for Molecular Sciences, State Key Laboratory of Polymer Physics and Chemistry, CAS Research/Education Center for Excellence in Molecular Sciences, Institute of Chemistry, Chinese Academy of Sciences, Beijing 100190, China

[c] Department of Chemistry, Southern University of Science and Technology, Shenzhen 518055, China

1.Synthesis

Unless stated otherwise, all the chemical reagents and solvents used were obtained commercially and were used without further purification. Chloroform, 1,2-dichloroeth were dried by molecular sieve and tetrahydrofuran (THF) were dries by sodium and distilled from sodium benzophenone under nitrogen. Compound 1 and compound 2 were synthesized according to the reported process.[1, 2]

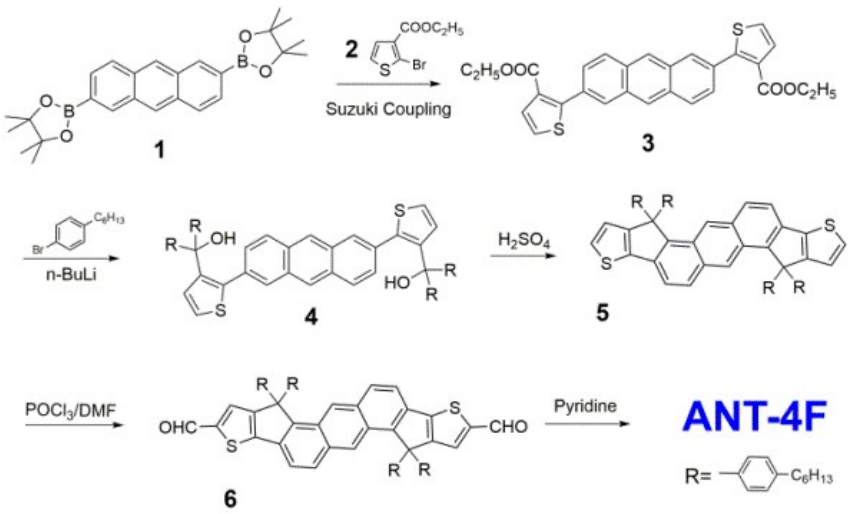

Figure S1.Synthesis routes of ANT-4F

Compound 3

Compound 1 (860 mg, 2 mmol), compound 2 (1.2 g, 5 mmol) were dissolved in anhydrous toluene (30 mL), ethanol(7.5 mL), 1M K_2CO_3 aqueous. Then $Pd(PPh_3)_4$ (69.3 mg, 0.06 mmol) was added, and the mixture was deoxygenated with nitrogen for 20 min. The solution mixture was stirred at 90 °C for 24 h, and then cooled to room temperature. 30 mL of water and 30ml of petroleum ether was added and the mixture was filtered. The residue was washed with water and acetone. After dried, the residue was obtained as a pale yellow solid (0.9 g, 82%) and directly used for next step.

Compound 5

To a solution of compound 3 (0.5 mg, 1 mmol) in dry THF (15 mL) under nitrogen was added 4-hexylbenzene 1-magnesium bromide (6 mL, 6 mmol) dropwise at room temperature. The resulting mixture was stirred at reflux for 12 h. The reaction solution was extracted with dichloromethane (50 mL × 3) and ammonium chloride solution (150 mL). The combined organic layer was dried over $MgSO_4$. After removal of the solvent under reduced pressure, a brown sticky solid was obtained and directly used for next step reaction without further purification. To a solution of compound 4a in octane (25 mL) was added acetic acid (6 mL) and sulfuric acid (0.1 mL) slowly. The resulting solution was stirred at 65 °C for 6 h. After removal of the octane under reduced pressure, the residue was extracted by sodium carbonate solution (50 mL × 3) and dichloromethane (50 mL×2). Then, the crude products were purified by column chromatography on silica gel using petroleum ether/dichloromethane (10:1) to give a yellow solid (0.35 g, 2 steps overall yield 60%).^{1}H-NMR (300 MHz, CDCl3): δ 8.24 (s, 2H), 7.80 (d, 2H), 7.60 (d, 2H), 7.25 (d, 2H), 7.2 (d, 8H), 7.06 (d, 2H), 7.02 (d, 8H), 2.51 (t, 8H),1.52 (t, 8H), 1.26 (s, 24H), 0.82 (t, 8H).

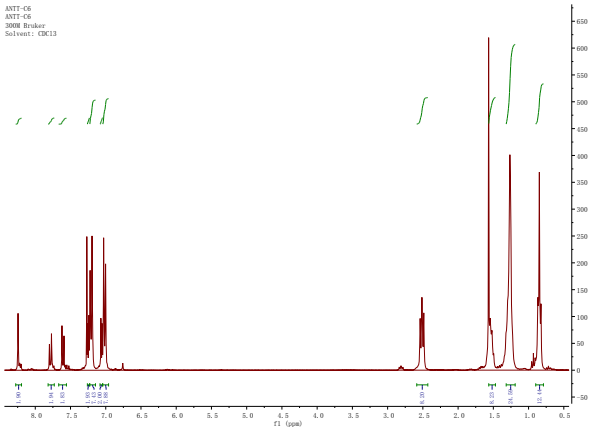

Compound 6

A Vilsmeier reagent, which was prepared with $POCl_3$ (0.10 mL) in DMF (3 mL), was added to a solution of compound 5a (0.35 g, 0.3 mmol) in 1,2-dichloroethane (25 mL) under the protection of nitrogen. After heating at 65 °C overnight, the mixture was poured into ice water (50 mL), neutralized with Na_2CO_3 (aq), and then extracted with dichloromethane (50 ml x 2). The combined organic layer was washed with water and brine, dried over anhydrous Na_2SO_4. After removal of solvent, the crude product was purified by silica gel using petroleum ether/dichloromethane (1:1) as eluent, yielding a yellow solid (0.3 g, 88%).^{1}H-NMR (300 MHz, CDCl3): δ9.8(s,2H), 8.32 (s, 2H), 7.86 (d, 2H), 7.70 (S, 2H), 7.68 (d, 2H), 7.2 (d, 8H), 7.07 (d, 8H), 2.53 (t, 8H),1.55 (t, 8H), 1.28 (s, 24H), 0.84 (t, 8H).

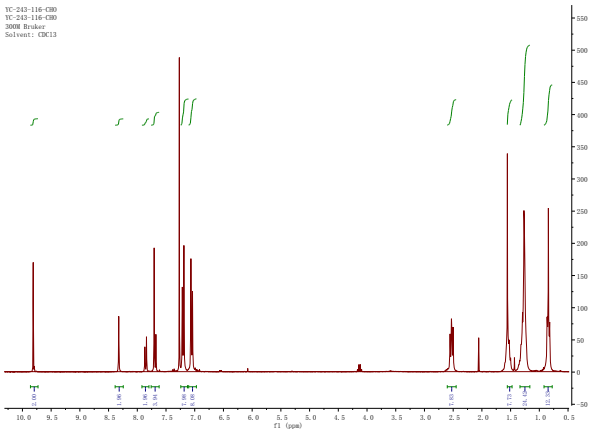

ANT-4F.

To a three-necked round bottom flask were added compound 6a(100 mg, 0.1 mmol), 2FIC (69 mg, 0.3 mmol), pyridine (0.1 mL) and chloroform (30 mL). The mixture was deoxygenated with nitrogen for 20 min and then stirred at reflux for 15 h. After cooling to room temperature, the mixture was poured into methanol (100 mL) and filtered. The residue was purified by column chromatography on silica gel using petroleum ether/dichloromethane (1: 1) as eluent yielding a dark brown solid (102 mg, 88%). ^{1}H-NMR (300 MHz, CDCl3): δ 8.85 (s, 2H), 8.53 (m, 2H), 8.32 (s, 2H), 7.91 (d, 2H), 7.8 (d, 2H), 7.76 (s, 2H), 7.7 (t, 2H), 7.21 (d, 8H),7.09 (d, 8H), 2.56 (m, 8H), 1.57 (m, 8H), 1.28 (m, 24H), 0.86 (m, 12H). MS (MALDI-TOF): m/z (M+). MS(MALDI): calcd for 1486.58; found: 1487.58. ^{13}C NMR (126 MHz, $CDCl_3$) δ 161.44, 158.45, 153.00, 142.30, 140.83, 139.16, 138.80, 137.39, 134.41, 132.37, 132.18, 128.74, 128.61, 120.94, 119.50, 115.06, 114.16, 92.47, 64.10, 35.49, 31.63, 31.09, 29.67, 29.05, 22.52, 13.99.

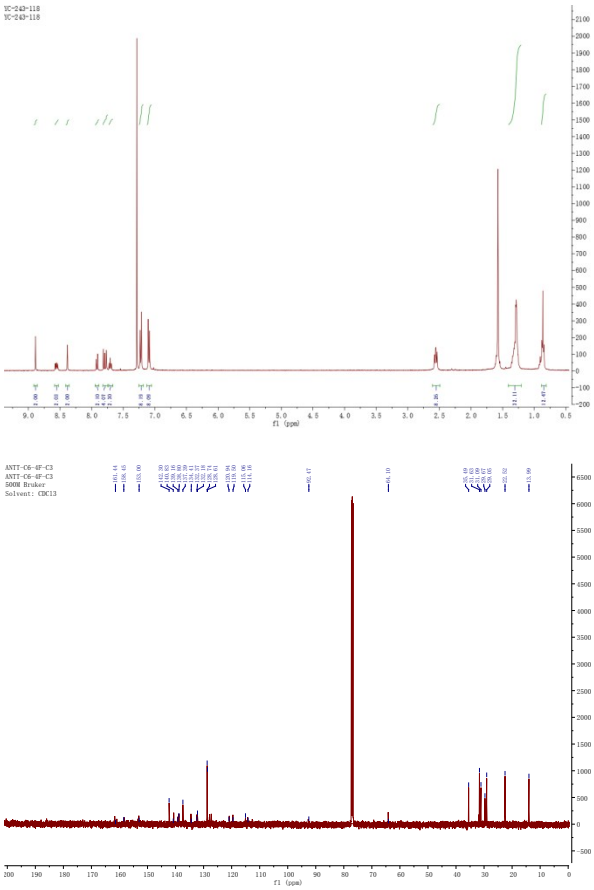

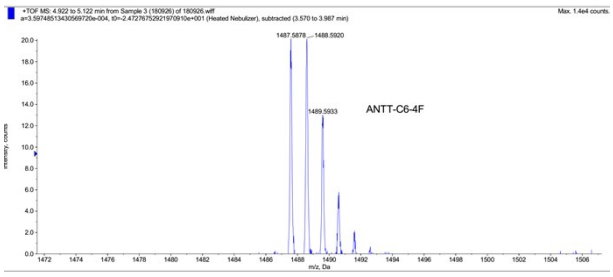

2.Characterization

The NMR spectra were measured using Bruker AVANCE 300 or 400 or 500 MHz spectrometer. Mass spectra were measured on a Bruker Daltonics Biflex III MALDI-TOF Analyzer in the MALDI mode. Solution (dichloromethane) and thin film (on a quartz substrate). UV-vis absorption spectra were recorded using a JΛSCO V-570 spectrophotometer. Electrochemical measurements were carried out under nitrogen in a solution of tetra-n-butylammonium hexafluorophosphate ([nBu4N]+[PF6]–) (0.1 M) in CH_3CN employing a computer-controlled CHI660C electrochemical workstation, glassy carbon working electrode coated with acceptor films, an Ag/AgCl reference electrode, and a platinum-wire auxiliary electrode. The potentials were referenced to a ferrocenium/ferrocene ($FeCp^{2+}/0$) couple using ferrocene as an internal standard. The transmission electron microscopy (TEM) characterization was carried out on a JEM-2100 transmission electron microscope operated at 200 kV. The samples for the TEM measurements were prepared as follows: The active layer films were spin-casted on indium tin oxide (ITO)/poly(3, 4-ethylenedioxythiophene):poly(styrene sulfonate) (PEDOT:PSS) substrates, and the substrates with the active layers were submerged in deionized water to make the active layers float onto the air-water interface. Then, the floated films were picked up on unsupported 200 mesh copper grids for the TEM measurements.

Atomic force microscopy (AFM) was performed using Multimode 8 atomic force microscope in tapping mode. The transmission electron microscopy (TEM) investigation was performed on Philips Technical G^2F20 at 200 kv. Space charge limited current (SCLC) mobility was measured using a diode configuration of ITO/PEDOT:PSS/donor:acceptor/MoO_3/Ag for hole mobility and ITO/ZnO/donor:acceptor/Al for electron mobility and fitting the results to space charge limited form, where SCLC equation is described by :

$$J_{SCLC} = \frac{9}{8}\varepsilon_o \varepsilon_r \mu_o \frac{V^2}{L^3}$$

where J is the current density, L is the film thickness of the active layer, μ_0 is the charge mobility, ε_r is the relative dielectric constant of the transport medium, ε_0 is the permittivity of free space (8.85×10^{-12} F m^{-1}), V is the internal voltage in the device (= V_{appl} - V_{bi}), where V_{appl} is the voltage applied to the device and V_{bi} is the built-in voltage due to the relative work function difference of the two electrodes. The hole mobility and electron mobility of the blended films were measured using the SCLC (space-charge-limited current) method. The ANT-4F/PBDB-TF blended films with 0.5% DIO exhibit high hole mobilities of 7.6×10^{-4} $cm^2V^{-1}s^{-1}$ and high electron mobility of 1.4×10^{-4} $cm^2V^{-1}s^{-1}$. ANT-4F/PBDB-TF blended films show balanced charge transport (μ_h/μ_e=5.4) so high FF of 74.7% was obtained in the ANT-4F-based OSCs.

3.Organic solar cell fabrication

The devices were fabricated with a structure of glass/ITO/ZnO/donor:acceptor/ MoO_3/Ag. The ITO-coated glass substrates were cleaned by ultrasonic treatment in detergent, deionized water, acetone, and isopropyl alcohol under ultra-sonication for 15 minutes each and subsequently dried by a nitrogen blow. ZnO electron transport layer was prepared onto the ITO glass through spin coating at 3000 rpm from a ZnO precursor solution, then the ZnO substrates were immediately baked in air at 200 ℃ for 30 min, the substrates were transferred into an argon-filled glove box. Subsequently, the active layer was spin-coated from the blend chlorobenzene solutions of donor and acceptor. The MoO_3 layer (ca. 10 nm) and Ag (ca. 80 nm) were successively evaporated onto the surface of the photoactive layer under vacuum (ca. 10^{-6} Pa). The current density-voltage (J-V) curves of photovoltaic devices were obtained with a Keithley 2400 source-measure unit. The photocurrent was measured under illumination simulated AM 1.5G (100 mW cm^{-2}) irradiation using a SAN-EI XES-70S1 solar simulator, calibrated with a standard Si solar cell. External quantum efficiencies were measured using Stanford Research Systems SR810 lock-in amplifier. The active area of the device was ca. 4.5mm^2.

4.Electroluminescence measurement and EQE_{EL} calculation

The electroluminescence measurement consisted of injecting current from the anode, then collecting the emitted photons as functions of wavelength. The injection current here was provided from a constant flow source by Keithley 2400. The emission spectrum was then collected by two fiber optical spectrometers (QE65 Pro and NIRQuest) which were linked using a Y-optical fiber. Emissions from 400–1050 nm were detected by QE65 Pro, and light emissions from 1050–1600 nm were detected by NIRQuest. The light emitting devices were fabricated using a converted structure of ITO/ZnO/donor:acceptor/MoO_3/Ag. The emissions intensity was measured using the light guide positioned close to the sample. The obtained EL spectra intensity was calibrated with the spectrum from a calibrated halogen lamp (LS-1-CAL). Finally, an EL spectrum indicating relationship between emission energy density and the emission wavelength was obtained as shown in Fig. 3(c).

The definition of EQE_{EL} is

$$EQE_{EL} = \frac{N_\nu}{N_e},$$

where N_ν is the emission photon number and N_e is the injected electron number.

$$N_\nu = \frac{E_{emission}}{E_{photon}} = \frac{P_{emission} \times T}{E_{photon}},$$

where $P_{emission}$ is the light emission power from device, T is time and E_{photon} is the average energy of one emission photon.

$$E_{photon} = \frac{hc}{\lambda},$$

where h is Planck's constant (6.63×10^{-34} J·s), c is the velocity of light (3×10^{8} m/s), and λ is average wavelength of emission light.

$$N_e = \frac{I \times T}{e},$$

where I is the applied current and e is the electron charge (1.6×10^{-19} C).

Finally, we have the EQE_{EL} calculation equation:

$$EQE_{EL} = \frac{P_{emission} \times \lambda \times e}{h \times c \times I}.$$

In case of ANT-4F/PBDB-TF-based solar cells, the integral area under the blue curve in Fig. 3(c) was calculated as 11.78 μW/cm^2 and the device area was 0.045 cm^2, so the calculated light emission power was 0.53 μW. According to the numerical aperture of the fiber (0.22), the solid angle (θ) of the collected light is 0.1539. Considering that the real emission solid angle of the device is 2π, the real light emission power ($P_{emission}$) of the device should be 0.53 μW times 2π/0.1539=21.64 μW. The average emission wavelength of the ANT-4F/PBDB-TF-based device was calculated as 947 nm, and the injection current here was 100 mA. According to the EQE_{EL} calculation equation, the EQE_{EL} of ANT-4F/PBDB-TF is calculated as 1.65×10^{-4}. In the case of IT-4F/PBDB-TF-based solar cells, the integral area under the blue curve in Fig. 3 (c) was calculated as 1.74 μW/cm^2 and the device area was 0.045 cm^2, so the calculated light emission power was 0.078 μW. The real light emission power ($P_{emission}$) of the device should be 0.078 μW times 2π/0.1539=3.18 μW. The average emission wavelength of the IT-4F/PBDB-TF-based device was calculated as 966 nm. According to the EQE_{EL} calculation equation, the EQE_{EL} of IT-4F/PBDB-TF is calculated as 2.4×10^{-5}.

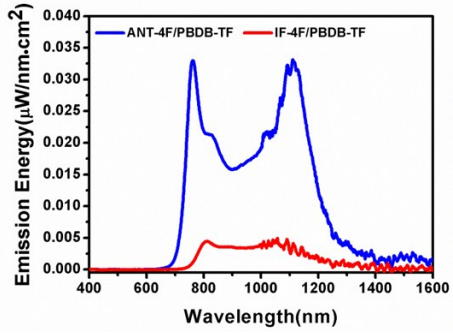

Fig 3.(c) EL spectrum of donor/acceptor blend films.

4.PLQY measurements

PLQY of ANT-4F and IT-4F are measured using HORIBA Instrument Incorparated Fluorolog-3. Diluted solution samples are prepared by dissolve little amount of materials into dry dichloromethane. The PLQY are calculated by instrumental system software.

To clearly demonstrate the improved fluorescence of ANT-4F is due to the anthracene core, two reported molecular structure similar NFSAs(IDT-4F and NT-4F) are compared.

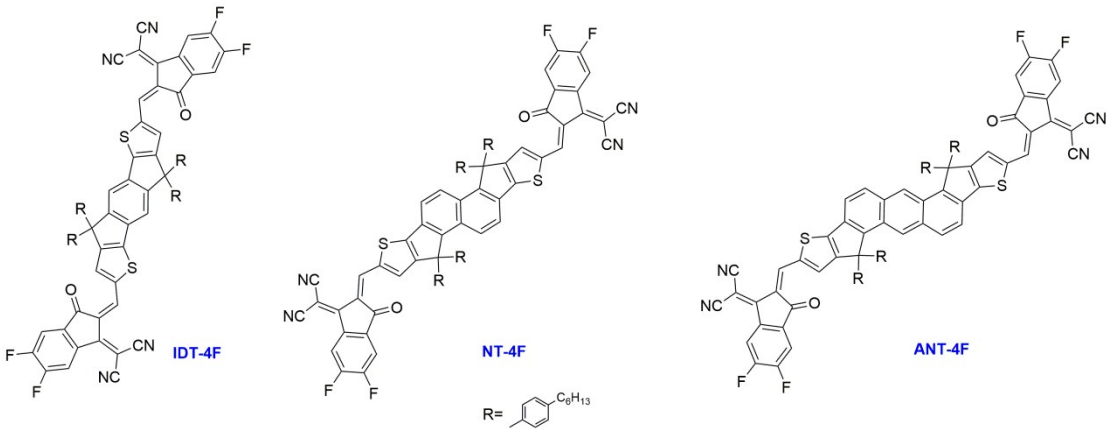

Figure S2.Molecular structure of IDT-4F, NT-4F, ANT-4F

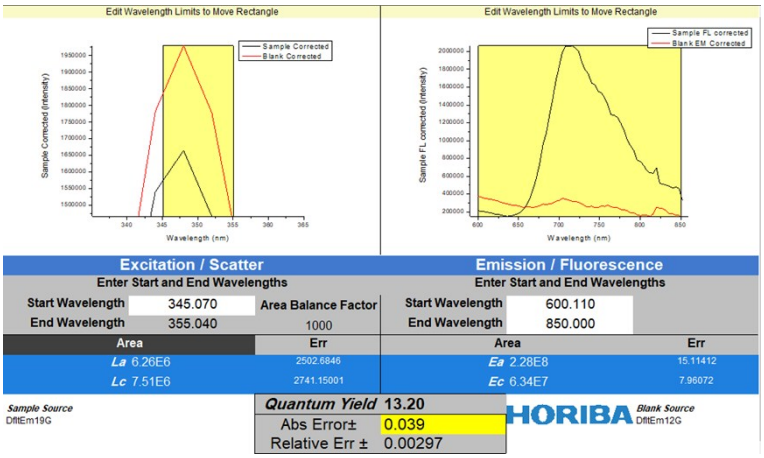

Figure S3(a).PLQY of IDT-4F

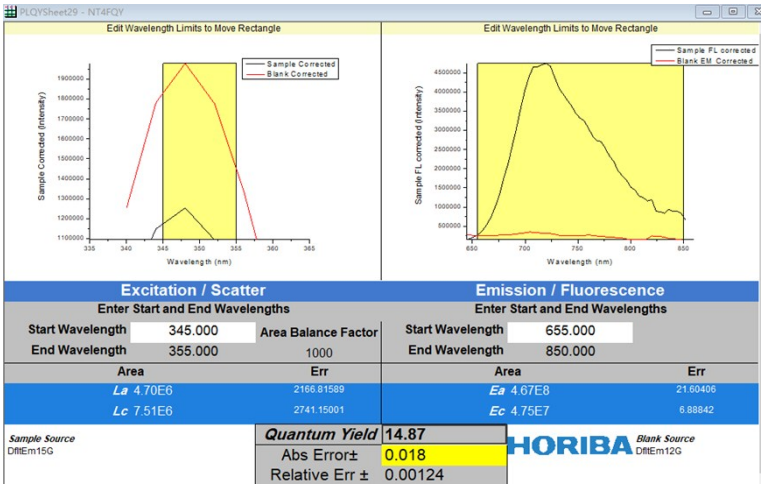

Figure S3(b).PLQY of NT-4F

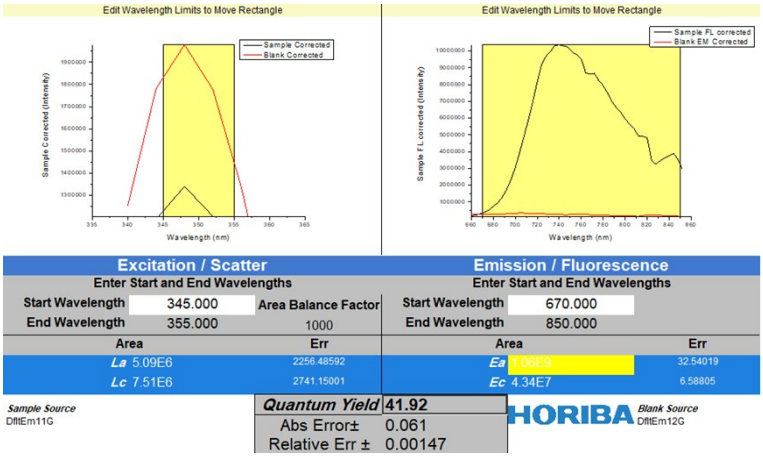

Figure S3(c).PLQY of ANT-4F

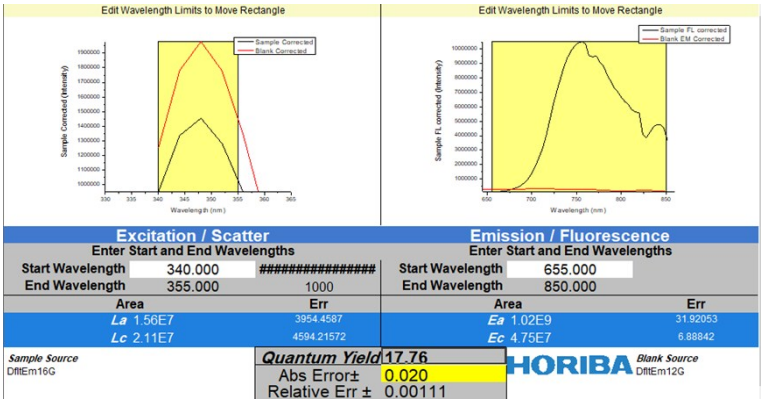

Figure S3(d).PLQY of IT-4F

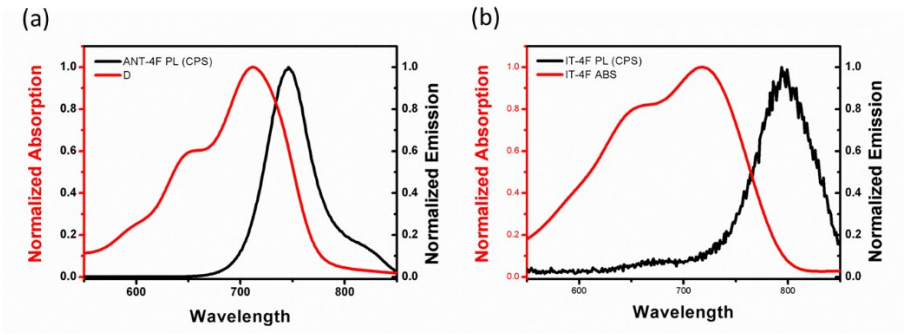

Figure S4.Crossing point of absorption spectrum and fluorescence emission spectrum

Optical band gap(Eg^{opt}) is calculated through the wavelength corresponding to the crossing point of absorption spectrum and fluorescence emission spectrum. Eg^{opt} for ANT-4F is 1.68 eV(738nm) and Eg^{opt} for IT-4F is 1.62 eV(765nm).

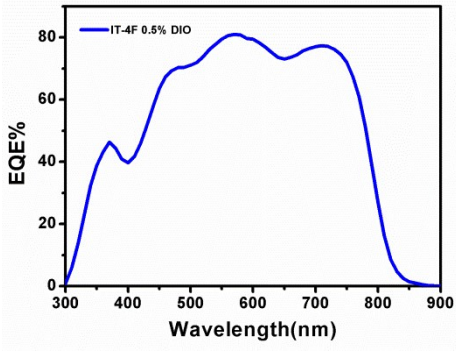

Fig S5. EQE curve of PBDB-TF/IF-4F based OSCs

Table S1

Photovoltaic performance of BHJ solar cells based on PBDB-TF/ANTT-C6-4F with donor concentration (CB, 10 mg/mL) and under illumination of AM 1.5 G 100 mW cm^{-2}. The active layer was casted from chlorobenzene solution with different PBDB-TF/ANTT-C6-4F weight ratios.

Weight ratio	Voc(V)	Jsc(mA/cm^2)	FF(%)	PCE(%)
1/0.8	0.89	16.4	66.1	9.6
1/1	0.95	16.9	71.7	11.5
1/1.2	0.90	16.7	70.5	10.6

Table S2

Photovoltaic performance of BHJ solar cells based on PBDB-TF/ANT-4F with donor concentration (CB, 10 mg/mL) and under illumination of AM 1.5 G 100 mW cm^{-2}. The active layer was casted from chlorobenzene solution with different DIO ratios

DIO ratio	Voc(V)	Jsc(mA/cm^2)	FF(%)	PCE(%)
0	0.95	16.9	71.7	11.5
0.25%	0.94	17.10	72.6	11.7
0.5%	0.94	17.6	74.7	12.3
1%	0.89	15.9	64.8	9.2

Table S3

Photovoltaic performance of BHJ solar cells based on PBDB-TF/ANT-4F with donor concentration (CF, 5 mg/mL, 6 mg/mL, 7 mg/mL,) and under illumination of AM 1.5 G 100 mW cm^{-2}.

Concertration (mg/mL)	Voc(V)	Jsc(mA/cm^2)	FF(%)	PCE(%)
5	0.93	16.9	72.5	11.4
6	0.94	18.1	71.3	12.1

7	0.92	17.6	68.2	11.1

Table S4

Photovoltaic performance of BHJ solar cells based on PBDB-TF/ANT-4F with DIO concentration (CF, 6 mg/mL, 0%, 0.25%, 0.5%) and under illumination of AM 1.5 G 100 mW cm^{-2}.

Concertration (%)	Voc(V)	Jsc(mA/cm^2)	FF(%)	PCE(%)
0	0.94	18.1	71.3	12.1
0.25	0.93	19.0	73.9	13.1
0.5	0.92	18.5	70.2	11.9

Table S5.

Hole and electro mobilities of different ANT-4F/PBDB-TF blend films

Acceptor	Electron mobility ($cm^2V^{-1}s^{-1}$)	Hole mobility ($cm^2V^{-1}s^{-1}$)
ANT-4F	1.4×10^{-4}	7.6×10^{-4}

1. Meng, H., et al., *High-Performance, Stable Organic Thin-Film Field-Effect Transistors Based on Bis-5′-alkylthiophen-2′-yl-2,6-anthracene Semiconductors.* Journal of the American Chemical Society, 2005. **127**(8): p. 2406-2407.
2. Bronstein, H., et al., *Synthesis of a Novel Fused Thiophene-thieno[3,2-b]thiophene-thiophene Donor Monomer and Co-polymer for Use in OPV and OFETs.* Macromolecular Rapid Communications, 2011. **32**(20): p. 1664-1668.